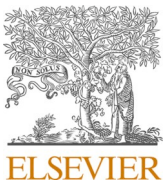




Since January 2020 Elsevier has created a COVID-19 resource centre with free information in English and Mandarin on the novel coronavirus COVID-19. The COVID-19 resource centre is hosted on Elsevier Connect, the company's public news and information website.

Elsevier hereby grants permission to make all its COVID-19-related research that is available on the COVID-19 resource centre - including this research content - immediately available in PubMed Central and other publicly funded repositories, such as the WHO COVID database with rights for unrestricted research re-use and analyses in any form or by any means with acknowledgement of the original source. These permissions are granted for free by Elsevier for as long as the COVID-19 resource centre remains active.



Research paper

Neuroprotective immunity by essential nutrient “Choline” for the prevention of SARS CoV2 infections: An in silico study by molecular dynamics approach

Papia Chowdhury ^{a,*}, Pustak Pathak ^b^a Department of Physics and Materials Science and Engineering, Jaypee Institute of Information Technology, Noida 201309, Uttar Pradesh, India^b Vishwa Bharati Public School, Arun Vihar, Noida, Sector 28, 201301, Uttar Pradesh, India

ARTICLE INFO

ABSTRACT

Keywords:

COVID-19
SARS-CoV2
 $3CL^{pro}$
Choline
RMSD
RMSF

Prenatal COVID infection is one of the worst affected and least attended aspects of the COVID-19 disease. Like other coronaviruses, CoV2 infection is anticipated to affect fetal development by maternal inflammatory response on the fetus and placenta. Studies showed that higher prenatal choline level in mother's body can safeguard the developing brain of the fetus from the adverse effects of CoV2 infection. Choline is commonly used as food supplement. By virtual screening, molecular docking and molecular dynamics techniques, we have established a strong inhibitory possibility of choline for SARS $3CL^{pro}$ protease which may provide a lead for prenatal COVID-19 treatment.

1. Introduction

A pandemic situation which has risen from the COVID-19 disease caused by a member of the coronavirus family of viruses, namely SARS-CoV2 is now been faced by the whole world. As coronaviruses are well known from last few decades, it's already understood that these viruses have specific enveloped RNA which can be the reason for various respiratory illnesses like common cold to fatal pneumonia of varying severity [1]. It was first found in domestic poultry in 1930s, and it was later recognized as cause of respiratory, liver, gastrointestinal, and neurologic diseases in animals [2]. Seven categories of coronaviruses are known, out of which four can only cause mild illness with symptom of common cold to the healthy human being. Severe lower respiratory tract infections and pneumonia for infants, immune-compromised patients and older people [3,4] can be caused by these viruses in very rare cases. The rest three categories: SARS-CoV (identified in 2003) [5], MERS-CoV (identified in 2012) [6] and SARS-CoV2 (identified in 2019) [7] can cause severe respiratory infections which can sometimes become fatal to the humans. Devastating and deadly outbreaks of SARS-CoV2 have already been observed in December 2019 in Wuhan, China [7,8]. The virus has been observed to spread worldwide within a few weeks of its appearance and to reveal its global presence by showing symptoms of respiratory illness (both acute and severe) caused by it [9]. It was soon

realized that in addition to usual respiratory problems, acute respiratory distress syndrome (ARDS) and death can also be caused by this virus. It's observed fact that the risk of death and/or serious symptoms due to COVID-19 increases in older people and in patients with other serious medical issues including obesity, diabetes, and heart, lung, kidney or liver disease [10]. The outcome of the above mentioned severity can progress to respiratory failure requiring mechanical ventilation, shock, multi organ failure, and death [11–14]. CoV2s are zoonotic pathogens in nature which usually appear in animals first. Due to the similarities of 79% and 96% for complete genome sequence recognition rates of SARS-CoV and bat SARS-CoV (SARSr-COV-RaTG13) it's suggested that bats may be the hosts of CoV viruses [15]. Similarly, for CoV2 there may exist original, intermediate and final hosts and so the disease may transfer from infected animal to human. For SARS-CoV2, person-to-person transmission is the easier way to spread the disease which can happen easily through infected secretions mainly via respiratory droplets, surface contaminated and possibly by aerosol transmission. Research outputs obtained till now have led to the conclusion that this virus can easily be transmitted by symptomatic, asymptomatic and presymptomatic patients [16–18]. As per latest reports, COVID-19 patients are mainly treated by providing supportive treatment only [19]. Around 200 FDA approved drugs and vaccines through clinical trials have been registered. Some investigational antiviral drugs like: Remdesivir,

* Corresponding author.

E-mail address: papia.chowdhury@jiit.ac.in (P. Chowdhury).

Favipiravir, Hydrochloroquine, Chloroquine, etc. have been in use for patients with severe symptoms [20,21]. However, toxicities associated with these drugs have already created some major fatal health issues [20]. Alternatively, some Immunomodulatory therapy by including convalescent plasma also are in use but as per today, specific drugs and vaccines to fight against COVID-19 are yet to be discovered or are still under development. As a part of this development, some particular nutrient food supplements and herbal medicines which specifically have some antiviral, immunomodulatory activities against different viruses like influenza, HIV, other coronaviruses can be considered with the aim of promoting the use of dietary therapy, hard immunity and herbal medicine as an alternative of COVID-19 therapies [22–24]. A set of research works have already suggested that nutrient food supplements and herbs possess a potential antiviral ability, hard immunity against SARS-CoV2 [23,24].

Previous pandemics due to different viruses have shown their effects on fetal developments which led to significant enhancement in number of infants with mental illnesses like schizophrenia, autism spectrum disorder and attention deficit disorder [25,26]. As per report of “The Centers for Disease Control and Prevention (CDC),” prenatal COVID-19 infections can also develop its impact on fetal brain development by the effects of the maternal inflammatory response on the fetus and placenta [10,26,27]. The supporting data regarding this impact of COVID-19 is expected to be available in near future. Current reported data from CDC based on Infant Behaviour Questionnaire Revised (IBQ-R) regulation [27,28] suggest that no symptoms of viral infections are found after 3 months of birth on the children of COVID-19 infected mothers having high digestive choline level ($\geq 7.5 \mu\text{M}$) during the first 16 weeks of pregnancy. Some specific diets and food supplements are the source of choline for human body. Medical reports suggested that higher choline level in expecting mothers may protect fetal brain development from COVID-19, which definitely may support infant behavioral development though the mothers got COVID-19 infection in their gestation stage when the brain is being formed [26–29]. These findings have motivated us to work on a specific nutrient food supplement: Choline ($\text{C}_5\text{H}_{14}\text{NO}$) which is supposed to be used to protect the fetal brain development specifically during pregnancy [27]. Our in silico studies by virtual screening, molecular docking and molecular dynamics on choline as ligand and 3CL^{pro} main spike protease of CoV2 as receptor have been able to establish that prenatal COVID-19 infections can be nullified by choline contained food supplements as they help to shield the fetal brain in mother’s womb from the possible detrimental impact from COVID-19 (Fig. 1a, b).

2. Materials and methods

2.1. Potential inhibitor choline

Choline is present in some dietary supplements/foods and belongs to the Vitamin B family. Choline is naturally found in many plant-based products like beans and cruciferous vegetables including dried nuts, whole grains, and seeds [30]. It's also found in animal-based products like poultry, dairy products, meat, eggs, and fish. It is one of the

phytoconstituents extracted from herbal plants like *tinospora cordifolia*, *withania somnifera* [23]. Choline is endogenously produced in human liver as phosphatidylcholine. However, the amount of endogenously produced choline is not enough to meet our needs [31]. Choline plays a very significant role in forming of human genes, various metabolism process, and lipid transport. Choline:Urea (1:2) eutectic mixture is used as a reaction medium known as deep eutectic solvent (DES) for different nucleic acids [32]. Due to its water free storage capacity the mixture can be used as reaction medium for different biocatalytic reactions and as long-term storage medium at high temperature also [33]. It can act as a nano-crowder to protect protein structure from denaturation [34]. It helps the cell membranes to connect and communicate within the whole body. Choline composed DES can be used in different enzymatic reactions to obtain the green chemical processes [35]. Choline is an important component of breast milk on which the fetal development of a child is dependent during the early birth stages. Medical studies reveal that proper intake of choline supplements by would be mothers can protect the infants from neurodegenerative diseases like Down syndrome, Alzheimer's diseases [36]. Choline is a direct precursor of Ach (acetylcholine) which is a neurotransmitter that controls a large number of autonomic, cognitive, and motor functions [36]. As per the medical studies, if choline is taken by the mother during pregnancy, this would make the newborn baby capable enough to mitigate the risks of CoV2 infections [26]. Reports also suggest that prenatal choline supplement is capable of brain development of unborn child by decreasing the effect of various viral respiratory infections like deficit disorder, schizophrenia including COVID-19 [26–28,37]. Like other coronaviruses, COVID-19 disease can destroy a child's respiratory organs and also hamper brain development adversely by inciting the maternal immune response [38,39]. As per Freeman et al higher maternal choline levels at 16 months gestation can diminish the effects of inflammation in the children's behaviors at 3 months of age [26–28]. Though the effects of choline in COVID-19 infection on infant development are still unknown, still all available medical data validate the fact that choline supplements may help to maintain the higher prenatal choline level to protect the early fetal brain development of the infants so that infants may survive in a healthy manner though the mother get affected by the CoV2 infection [40,41]. However, not much research justifying this hypothesis has been conducted until now. Rigorous investigation is still needed to explore the connection between choline and SARS CoV2 infections and to determine whether choline can act as a potential inhibitor against the receptor protein CoV2 main protease and to be used as potential drug so that choline supplements might benefit patients with COVID-19 disease. For understanding the stability and activity of a specific inhibitor on a receptor enzyme at different experimental conditions is known as bottleneck for successful drug designing. Counteraction effects of choline as DES mixture have already proved their effectiveness in maintaining native conformational stability and activity of proteins and enzymes in aqueous solutions [42,43]. For the present study we have downloaded the structure of choline in PDB format from Drugbank (<https://www.drugbank.ca/drugs>) (Fig. 1b). We have also done the proper virtual screening by evaluating their drug-likeness, pharmacokinetics and lipophilicity properties which are a set of guidelines for

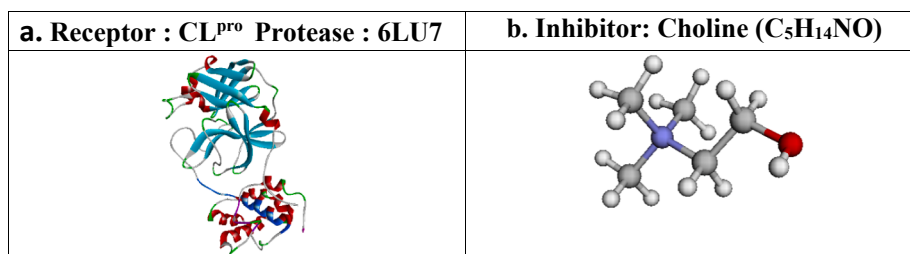


Fig. 1. (a) Structure of receptor protein (6LU7). (b). Structure of Choline.

identification of potential drug compounds (Table 1). Some mostly industry applicable drug-likeness rules are: "Lipinski's rule", "MDDR-like rule", "Veber's rule", "Ghose filter", "Egan rule", "Muegge rule", etc [44–47]. SWISS-ADME software (<https://www.swissadme.ch>) has helped us in applying different virtual screening methods. For Molecular docking study, ligand choline has been saved in pdbqt format by Auto Dock Tools 1.5.6 [48].

2.2. Potential target protein structure for SARS-CoV2

Corona virus encodes large number of structural and nonstructural polyproteins. Among them some polyproteins become cleaved and transformed themselves into some mature nonstructural protein by protease 3CL^{pro} which is a key to SARS-CoV enzyme [49]. Cov 3CL^{pro} is responsible for controlling functions replication and transcription processes by its spike (S) glycoprotein [50]. S enters the host cell and from the viral surface it forms homo trimers. After entering it interacts strongly with the ACE2 (angiotensin-converting enzyme 2) receptor and replicates itself through some cyclic processes [51]. Targeting 3CL^{pro} protease may constitute a valid approach for anti COVID drug designing. 3D structure of one of the 3CL^{pro} like protease protein is reported by X-Ray crystallographic data (PDBID: 6LU7) [52] (Fig. 1a). We have checked the inhibiting and binding possibilities of this natural 3CL^{pro} like protease protein substrate in order to find the effectiveness of choline against COVID-19 in the present work. The structure of 6LU7 was downloaded from the "Protein Data Bank" (<https://www.rcsb.org/>) and has been prepared for further simulation purposes by Auto Dock and MG Tools of Auto DockVina software [53]. The inbuilt ligands were removed from 6LU7 using Discovery studio 2020 (Dassault Systèmes BIOVIA) [54] and the output structure was subsequently cleaned and saved in PDB format.

2.3. Methods: molecular docking, molecular dynamics, binding energy

Molecular docking which performs energy minimization and binding energy calculations, is one of the most applied simulation mechanisms used to predict the potential drug-target interactions. It can identify the best orientation/pose of ligand towards host protein. Docking algorithms with the help of some scoring functions are used to identify the suitable ligand conformation at energy minimized state [55]. Molecular docking can predict whether the ligand/drug is docked with the receptor protein/DNA or not and show the results in the form of rankings of docked compounds which are dependent on lower binding energy. The algorithm of AutoDock Vina with some best fitted configuration parameters (binding modes- 9, exhaustiveness – 8, energy difference- 3 kcal/mol, Gridbox center with coordinate x, y, and z of residue position of the target protein) is used to do the docking-based studies on the

suggested inhibitor onto the protease of CoV-2 [53]. The target protein is saved in pdbqt format by Auto Dock Tools [53] and ready to be used for docking. After simulation, the pose showing maximum nonbonded interactions, dipole moment with minimum binding affinity (kcal/mol), drying energy, inhibition constant was chosen as the best ligand: protein complex structure. Another criteria of choosing best ligand: protein pose is identifying the types and number of bonding between them. The metabolite which makes maximum number of H-bonds, electrostatic bonds with the receptor protein mostly show better capability to form ligand: protein complex.

MD simulation results helped us to investigate the structural dynamics of protein: ligand interactions. LINUX based platform "GROMACS 5.1 Package" [56] with CHARMM36 all atom [57] and GROMOS43A2 force fields [58] are used for determination of various thermodynamic parameters like potential energy (E_{pot}), temperature (T), density progression (D), radius of gyration (R_g), root mean square deviation (RMSD) for backbone, root mean square fluctuation (RMSF) for protein C_α backbone, solvent accessible surface area (SASA), hydrogen bonds, interaction energies of the proposed ligand: protein complex. CHARMM36 is all atom type which is additive in nature including parameters for proteins, nucleic acids, lipids, carbohydrates and drug-like biomolecules. Here the atomic partial charges are derived from quantum chemical calculations of the interactions between model compounds and water. Whereas GROMOS43A2 is a united atom force field without explicit aliphatic (non-polar) hydrogens applied mainly for biomolecular system. Here the smallest interacting unit is group of atoms of the system. Choline was optimized by Gaussian 9.0 by Density Functional Theory (DFT) with the basis set 6.31G (d,p) [59,60]. TIP3P water model and steepest descent algorithm has been used for energy minimization of the system in two steps each with varying time (1–10 ns) for 500,000 iteration steps with a cut-off up to 1000 kJmol⁻¹ for reducing the steric clashes. For the present work we have decided to stick upto 10 ns simulation since we have observed that within 10 ps of the time scale trajectory, both 6LU7 and choline: 6LU7 have reached to it stability. In first step, a boundary condition of constant number of particles (N), volume (V), and temperature (T) has been applied and in second step, it was constant NPT (particle numbers, pressure, temperature) under the pressure of 1 atmosphere and temperature 298 K. For the nonbonded interactions, short range Lennard-Jones and Coulomb interaction have been used. After final step of each simulation, obtained trajectories and results were analyzed using the graphical tool Origin pro. Detailed major information of MD simulation, docking, virtual screening study with constituents, time required, salvation box length etc are same as our previous work [24] and references therein.

To compute the interaction free energies of protein: ligand complex (ΔG_{bind}), we have used Molecular Mechanics Poisson-Boltzmann Surface Area (MMPBSA) method [61] sourced from the GROMACS and APBS

Table 1

Physiochemical, Drug-likeness, pharmacokinetics and lipophilicity properties, Medicinal chemistry of choline.

Properties of Choline (C ₅ H ₁₄ NO)									
Physicochemical Properties	choline	Lipophilicity	choline	Druglikeness	choline	Pharmacokinetics	choline	Medicinal Chemistry	choline
Molecular weight (gm/mol)	104.1708	Log $P_{o/w}$ (iLOGP)	-2.41	Lipinski	yes	GI absorption	Yes	PAINS	0 alert
Num.H-bond acceptors	1	Log $P_{o/w}$ (XLOGP3)	-0.40	Veber	yes	BBB permeant	No	Brenk	1 alert
Num. H-bond donors	1	Log $P_{o/w}$ (WLOGP)	-0.32	Ghose	Partly yes (2 violation)	P-gp substrate	No	Leadlikeness	Partially yes (1 violation)
No of rotatable bonds	2	Log $P_{o/w}$ (MLLOGP)	-3.46	Egan	yes	Log K_p (skin permeation)	-7.22 cm/s	Mutagenicity	No
Molar Refractivity	29.69	Log $P_{o/w}$ (SILICOS-IT)	-0.57	Bioavailability score	137.87	Water Solubility	-1.26	Liver and cardio cytotoxicity	No
Topological polar surface area TPSA (Å ²)	20.23 Å ²	Concensus Log Po/w	-1.38	Synthetic accessibility (SA)	1.00	Log S (SILICOS-IT)	5.74e + 00	The Maximum Recommended Therapeutic Dose (MRTD)	5.2 mg/day

packages. The model contains both repulsive and attractive components [62]. The snapshots at every 100 ps between 0 and 10 ns were collected to predict the binding energy. The binding free energy of the bound ligand: receptor complex in aqueous solvent can be expressed by following equations:

$$\Delta G_{bind,aqu} = \Delta H - T\Delta S \approx \Delta E_{MM} + \Delta G_{bind,solv} - T\Delta S. \quad (1)$$

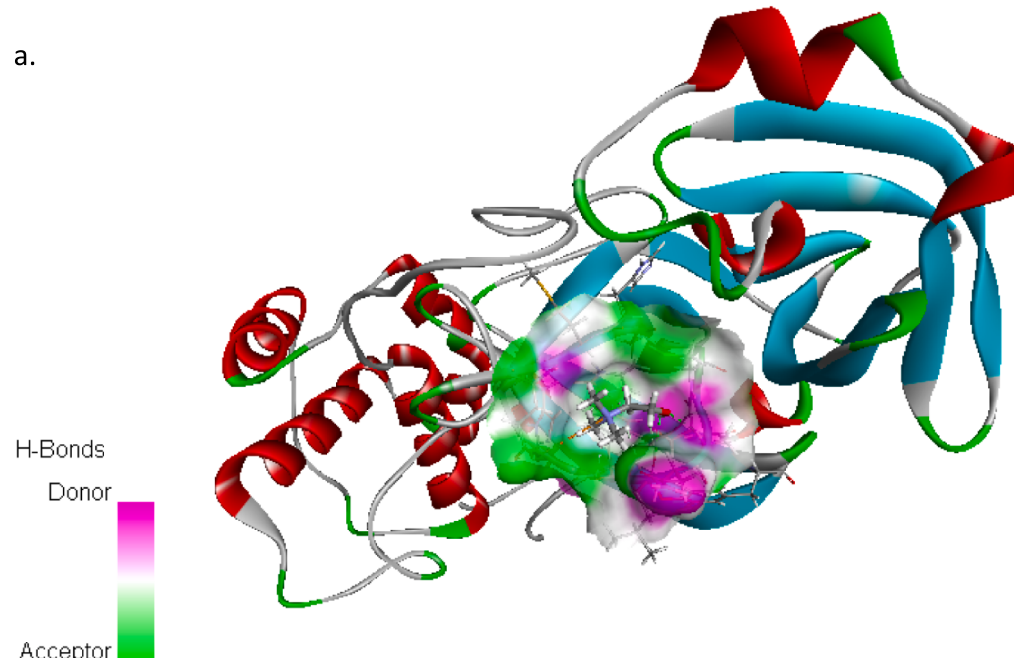
$$\Delta E_{MM} = \Delta E_{covalent} + \Delta E_{electrostatic} + \Delta E_{Van\;der\;Waals} \quad (2)$$

$$\Delta E_{covalent} = \Delta E_{bond} + \Delta E_{angle} + \Delta E_{torsion} \quad (3)$$

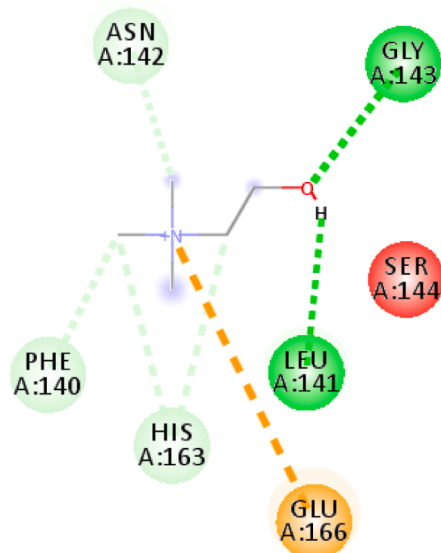
$$\Delta G_{bind,solv} = \Delta G_{polar} + \Delta G_{nonpolar}, \quad (4)$$

where ΔE_{MM} , $\Delta G_{bind,solv}$, $-T\Delta S$ are the molecular mechanical energy changes in gas phase, solvation free energy change and conformational energy change due to binding, respectively. ΔE_{MM} is the combination of covalent, electrostatic and Van der Waals energy changes. Covalent energy is the combination of bond, angle and torsion. $\Delta G_{bind,solv}$ is separated into its polar and nonpolar contribution. The entropy term is approximated with a normal mode method using a few selected snapshots. For binding free energy calculation, the MMPBSA method usually begins after the MD simulation of the complex using the single-trajectory approach [63].

a.



b.



Green: conventional hydrogen bond
 Sky blue: carbon hydrogen bond
 Yellow: attractive electrostatic bond

Fig. 2. (a) Donor: acceptor surface for hydrogen bonds for choline: 6LU7. (b). Possible types of interactions in best pose structure obtained from molecular docking for choline: 6LU7.

2.4. Computational facility

For the MD simulation and g_MM/PBSA computation works we have used Dell Gen 10 system (8 Core i5 processors) with 8 GB of RAM.

3. Results and discussion

3.1. Analysis of drug likeness properties of choline

The inhibition properties of probe molecule choline have been studied through SWISS ADME software to determine physicochemical descriptors and to predict ADME (Adsorption, Distribution, Metabolism and Excretion) parameters: pharmacokinetic properties, drug like nature and medicinal chemistry friendliness [64]. From the data mentioned in Table 1 we can see that choline was satisfying the most prescribed virtual screening properties like Ro5 as it has molecular weight less than 500 g/mol, TPSA values less than 40 Å². H-bond donors ≤5, H-bond acceptor 10, synthetic accessibility count between less than 5 so that they can be synthesized easily. It also follows Veber rule that means it satisfies all the bioavailability conditions. Its pharmacokinetics validate its neuroprotective role for the brain development. All medicinal chemistry parameters suggest that choline has no liver cytotoxicity effect in terms or drug induced liver injury for humans, null mutagenicity reveals that choline can cause no abnormal genetic mutations leading to cancer. It has no cardio toxicity also. According to ADMET (<https://vn nadmet.bhsai.org/>) data the maximum recommended therapeutic dose is 5.2 mg/day.

3.2. Analysis of molecular docking results

For receptor protein: 6LU7 and potential inhibitor: choline, docking result showed best 9 suitable pose structures for the choline: 6LU7 complex with their RMSD/ub (upper bound) and RMSD/lb (lower bound) variations. For pose 1 we obtained highest negative value of binding energy (-3.7 kcal/mol), lowest value of complex dreiding energy (104.198), and lowest value of inhibition constant ($k_i = 1.92 \times 10^{-3}$ M) at room temperature (298 K) as the best fit structure of ligand: receptor complex (Fig. 2, Table 2). We have repeated the docking simulation several times and got the variation in binding affinity for the best pose structure in between -3.7 kcal/mol to -3.4 kcal/mol. Usually, the dreiding energy values for individual protein and ligand are found to be different, but when they form complex the dreiding energy of the complex is found to be smaller than that of the individual protein and ligand. The complex structure having minimum dreiding energy corresponds to the most favourable structure [65]. In the same way for the best pose (1) structure the lowest k_i value proved the higher affinity of choline towards receptor 6LU7. The computed k_i value is far lower than

the toxicity dose range of choline (Table 1) which validate the strong candidature of choline as a proposed drug for CoV2 infection. Maximum value of dipole moment (5.374 debye) for pose 1 also validate the possibility of better complexation between choline and 6LU7 which arises due to the existence of strong electrostatic interaction (attractive type) between 6LU7 residue GLU166 and positively charged nitrogen (N1) of choline. Again, the weak hydrogen bonded interactions have significant role in defining the stability of protein: ligand complex as larger the number of nonbonded interactions the more is the possibility of binding affinity in ligand: protein complexation and so the possibility of formation of complex structure [66]. Maximum number of weak interactions (both conventional hydrogen bonds and carbon hydrogen bonds) were observed for pose 1 of docked structure between 6LU7 (Residues: GLY143, LEU141, HIS163, PHE140, ASN142) and choline (atoms: O1, H15, C4, C2, C3) (Fig. 2a, b, Table 2). In supporting document1 (SD1) we have presented the data for the two more suitable nearest docked poses which justifies the choice of pose 1 as best pose structure. So molecular docking results indicate that choline can be easily inhibited inside the favourable pocket of 6LU7 protein and can form a stable choline: 6LU7 complex by strong electrostatic bonding and weak hydrogen bonding between them. Existence of strong interaction between choline and 6LU7 have been established by MD simulation results in next section.

3.3. Analysis of molecular dynamics (MD) simulation results

As per protocol of MD simulation, we have used the TIP3P water model to fulfill the solvation process in a cubic box of the current choline: 6LU7 complex by adding 4Na⁺ external ions to maintain the neutrality of the present structure (Fig. 3a). For MD simulation, used force field is one of the important parameters to estimate the intramolecular forces within the molecule and intermolecular forces between molecules which helps to calculate the potential energy of the system of atoms or molecules. The decomposition of the terms in the used force fields (CHARM36 and GROMOS43A2) in terms of energy as:

$$E_{total} = E_{bonded} + E_{nonbonded} \quad (5)$$

$$E_{bonded} = E_{bond} + E_{angle} + E_{dihedral}. \quad (6)$$

$$E_{nonbonded} = E_{hydrogen\ bond} + E_{electrostatic} + E_{Van\ der\ Waals} \quad (7)$$

$$E_{electrostatic} = E_{coulombic} + E_{lenard\ Jones} \quad (8)$$

To quantify the strength of interaction between protein and ligand, nonbonded electrostatic interaction plays a vital part. For nonbonded interaction, we are interested mainly on short range electrostatic part. The whole MD simulation is performed under the varying time scale

Table 2

Various parameters like binding affinity, hydrogen bonded interaction, electrostatic interaction, dipole moment, drieding energy, inhibition constant for best docked pose structure for choline: 6LU7 complex.

Ligand	Best Binding affinity (kcal/mole)	Hydrogen bonded interaction (donor: acceptor, distance in Å) [Type of bond]	Electrostatic interaction (ligand donor: proton acceptor, distance in Å) [Type of bond]	Dipole moment of ligand (debye)	Drieding energy between protein and ligand	Inhibition constant (M)
choline	-3.7	(A:GLY143:HN - :PYA0:O1, 2.53816) [Conventional Hydrogen Bond] (:PYA0:H14 - A:LEU141:O, 2.6499)[Conventional Hydrogen Bond] (:PYA0:C4 - A:HIS163:NE2, 3.58031) [Carbon Hydrogen Bond] (:PYA0:C2 - A:PHE140:O, 3.6244) [Carbon Hydrogen Bond] (:PYA0:C2 - A:HIS163:NE2, 3.54655) [Carbon Hydrogen Bond] (:PYA0:C3 - A:ASN142:OD1, 3.243) [Carbon Hydrogen Bond]	(::PYA0:N1- A:GLU166:OE2, 5.10169)[Attractive Charge]	5.374	104.198	1.92×10^{-3}

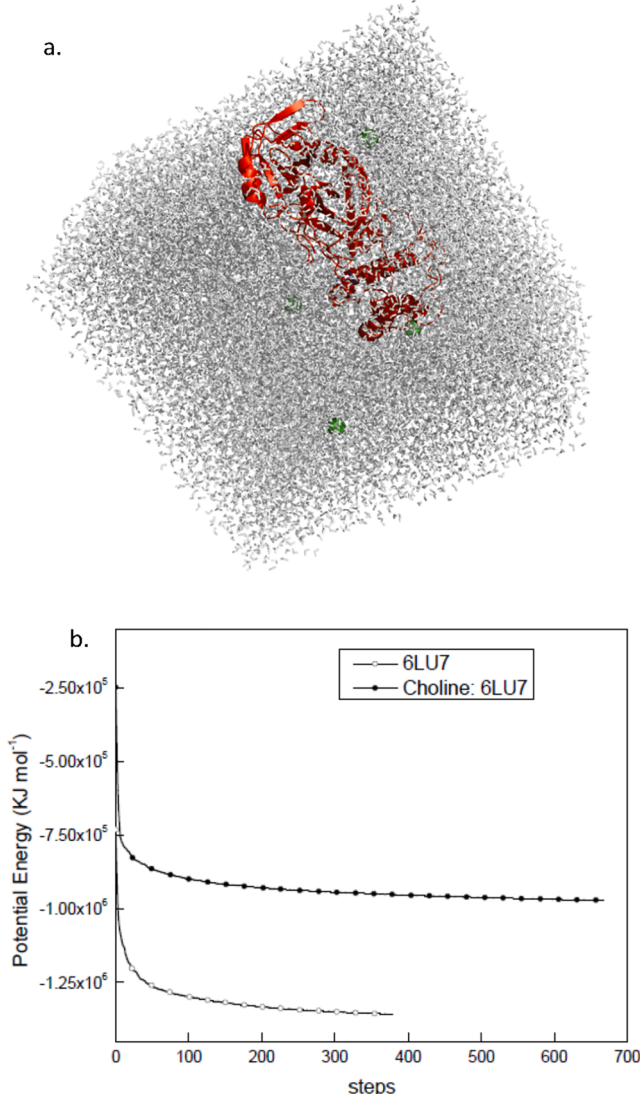


Fig. 3. (a) Solvated and neutralized choline: 6LU7 complex system in presence of water environment Na^+ ions. (b) Potential energy surface for optimized geometries of choline: 6LU7 complex and bare 6LU7.

from 10,000 ps to 100 ps. First, we have studied the stability of each structures (host and complex). We have optimized the probe systems by energy minimization process to get the minimum potential energy for both. For energetically stable structures, we obtained steady convergence of potential energy with negative energy minimum and maximum force value (Fig. 3b). For 6LU7 the computed average energy was $-1.27 \times 10^6 \pm 56.7$ (kJ mol⁻¹) for E_{pot} , while for choline: 6LU7 it was $-8.2 \times 10^5 \pm 38.77$ (kJ mol⁻¹). We have observed same order of results (energy, enthalpy, temperature, pressure density, volume, rmsd) both for 6LU7 and choline: 6LU7 complex in both CHARM36 and GROMOS43A2 force fields which justifies the applicability of any one of the force field (SD2a,b). For rest the simulation we have used GROMOS43A2. Further to check the stability of the structures under NVT and NPT equilibrated ensembles, we have tried to compute T, D, P, V of the probe systems within a varying time trajectory 100–10,000 ps. Simulated progression data showed that temperature of each system (receptor, complex) reached to a stable value (298 K) very quickly (within 100 ps) and maintained the stability throughout the whole simulation process for both applied force fields CHARM36 and GROMOS43A2 (cf. Fig. 4a). This also proved the applicability of both force fields for MD simulation. Same type of stability has been observed for density, pressure, volume

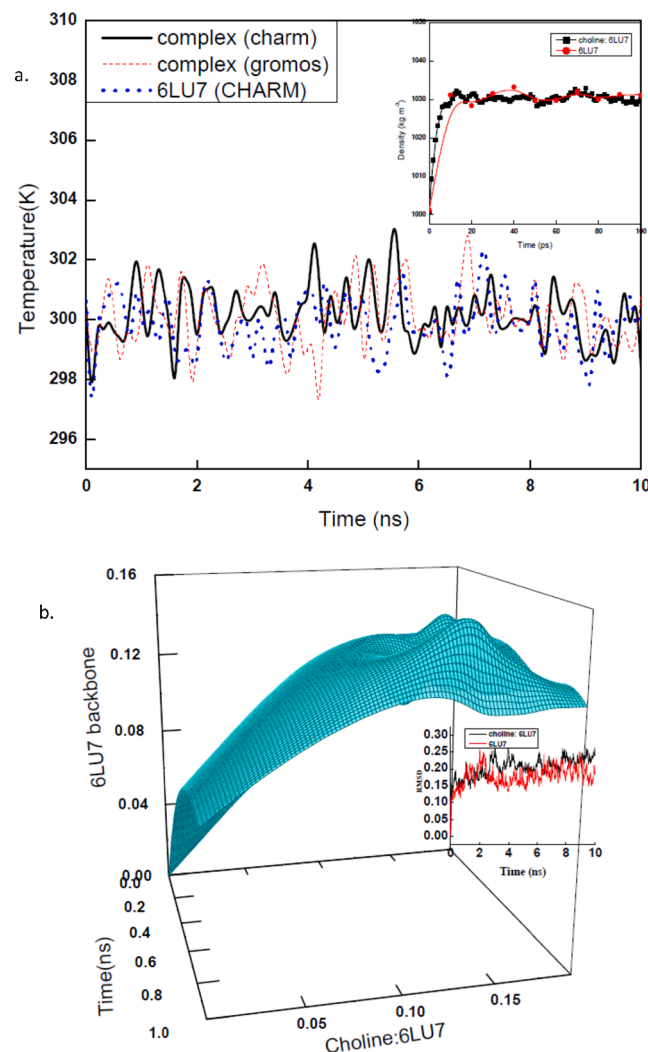


Fig. 4. (a) Temperature and density (inset) progression data for bare 6LU7 and choline: 6LU7 complex in water environment in CHARM 36 and GROMOS force fields. (b) Root mean square Deviation (RMSD) backbone graphs of 6LU7 in its bare state and in complex with choline (3D view upto 1 ns, 2D view upto 10 ns).

throughout the varying time scale (Inset of Fig. 4a). After running the whole simulation process we have computed several thermodynamics parameters of choline: 6LU7 complex in comparison to bare 6LU7 to understand the possible conformational arrangements during complexation throughout the whole time trajectory. The parameters are RMSD, RMSF, nonbonded interaction energy, hydrogen bonds, R_g , etc. (Table 3) [67]. RMSD is used to check the stability of host protein due to ligand binding with respect to the reference backbone structures of protein. Fig. 4b has shown the RMSD values of carbon backbone for choline: 6LU7 complex with respect to 6LU7 for the time scale trajectory up to 1 ns in 3D view (Fig. 4b). For better understanding a 2D diagram is also provided in the inset of Fig. 4b for larger time trajectory 1–10 ns. It is observed that RMSD for complex showed a variation between 0.14 and 0.26 (± 0.01) nm compared to 6LU7 variation 0.12–0.18 (± 0.01) nm which indicate the possibility of structure fluctuation during choline binding. The larger fluctuation in complex structure mainly arises between 7.5 ns and 10 ns time scale. Still the closeness between the average RMSD values of complex (0.18 nm) with host 6LU7 (0.16 nm) validated the stable docked choline: 6LU7 formation. Flatness in the 3D contour plot suggest that CL^{PRO} has shown no significant change in presence of choline during time resolved simulation. The contour plot also revealed steady phase of RMSD after 1 ns of the time trajectory. Similarly for RMSF, residue fluctuations of 6LU7 in complex were found

Table 3

Statistical data obtained by Molecular dynamic simulations for 6LU7 in its bare state without any ligand and in the complex state with ligand choline with GROMOS43A2 force field.

Serial no	Parameter	Bare 3CL ^{PRO} protease (6LU7)		6LU7 + choline complex	
		Mean	Range	Mean	Range
1.	SR Columbic Interaction energy (kJ mol ⁻¹)	NA	NA	-50.776 ± 20.12	-70 to -10
2.	SR LJ Interaction energy (kJ mol ⁻¹)	NA	NA	-95.26 ± 22.10	-30 to -120
3.	Average Interaction Energy energy (kJ mol ⁻¹)	NA	NA	-160.95 ± 20	NA
4.	RMSD (nm)	0.16 ± 0.01	0.12–0.18	0.18 ± 0.01	0.12–0.26
5.	Inter H-Bonds	NA	NA	2.5	0–6
6.	Radius of gyration	2.25 ± 0.01	2.25–2.26	2.25 ± 0.01	2.25–2.26
7.	SASA (nm ²)	22	19–26	19	16–20
9.	Potential Energy (kJ mol ⁻¹)	$-1.27 \times 10^6 \pm 56.7$	-7.3×10^5 to -1.3×10^6	$-8.5 \times 10^5 \pm 38.77$	-5.4×10^5 to -1.0×10^6
10.	Binding Energy (ΔG) (kJ mol ⁻¹)	NA	NA	-33.497 ± 27.406	NA
11.	Van der Waal Energy (ΔE_{vdw}) (kJ mol ⁻¹)	NA	NA	-34.656 ± 24.958	NA
12.	Electrostatic Eenergy (ΔE_{elec}), (kJ mol ⁻¹)	NA	NA	-7.380 ± 11.506	NA
13.	Polar solvation Energy (ΔE_{polar}) (kJ mol ⁻¹)	NA	NA	12.790 ± 28.852	NA
14.	SASA Energy (ΔE_{apolar} kJ mol ⁻¹)	NA	NA	-4.251 ± 3.148	NA

to be very small with respect to the 6LU7 in terms of C_α carbon. Closeness and less fluctuations in RMSF values suggest that choline: 6LU7 docked complex structure has not affected the host protein structure which remained mostly unaltered during simulation (SD3). To check it further we have analyzed the radial distribution function g(r) of choline and water around protein backbone which gives an average picture of the distribution of water or choline around the protein. The g(r) values of water and choline are presented in SD4. Figure SD4 suggests that water has a sharp increment at ~0.44 nm of the protein backbone. Beside this water shows a steady increment throughout the radial distribution. Whereas in presence of choline a sudden increment of peak height is observed. This sudden increment is definitely due to the repulsion between water and choline molecules. The change may be due to the fact that choline tries to preserve the compactness of the protein structure by repelling the water molecules towards protein backbone. The fact justifies the lower interaction possibility of choline with protein backbone.

To justify the above fact, we have computed Kirkwood G factor (SD 5) of water or choline around the protein backbone. Variation of Kirkwood G factor validate the net decrease in protein-choline interaction compared to protein-water interaction. Increment of G factor in protein-water clearly indicates increase of water density around protein. Similarly decrement of G factor in choline-protein indicates the influence of choline on the dynamics of water as water density around protein increases and so choline gets excluded from the protein backbone.

The radius of gyration (R_g) of a protein ligand complex or basic backbone protein gives us the hint of compressed nature of the probe system [68]. Variation of R_g values over the whole-time trajectory showed that the host 6LU7 and choline: 6LU7 complex showed a quite stable and compressed structures without lacking any major expansion/contraction throughout the simulation period. Both complex and base protein structures have reported R_g values between 2.25 and 2.26 nm with an average value of 2.25 ± 0.01 nm (SD6). Currently mostly used anti-COVID-19 drugs are Remdesivir, Favipiravir, hydrochloroquine. In Remdesivir the average R_g value is reported to be 2.2 ± 0.1 nm [69]. Favipiravir and hydroxychloroquine are also expected to show similar compactness due to their similar type of binding affinity towards 3CL^{PRO} protease as per Ref. [70]. The value of Remdesivir exactly matches with the average R_g value obtained for choline. This justifies the candidature of choline as a proposed CoV2 inhibitor. Similarly, SASA measures the area of receptor exposure to the solvents during the simulation process. In present study for 6LU7, SASA value was obtained between 19 and 26 nm² with a mean value of 22 nm² whereas for choline: 6LU7 complex, it was observed between 16 and 20 nm² with a mean value of 19 nm² (SD7). The closeness of the observed SASA values of both bare 6LU7 and its complex justified that ligand binding does not affect the folding of the receptor protein very much.

Though weaker than ionic and covalent interaction, intermolecular

hydrogen bonded interaction is a predominant contributor for complex formation. 3.5 Å cut-off condition has been used to find number of hydrogen bonds. In the present study we have observed a variation of number of hydrogen bonding between 0 and 6 throughout the whole-time trajectory with an average value of ± 2.6 (SD8). Obtained numbers perfectly matches with the molecular docking results and further validate the stability of choline: 6LU7 complexation. Short-range nonbonded interaction energy used to quantify the strength of the interaction between components of a complex. For the present case we have presented the variation of short-range Coulombic interaction energy and short-range Lennard-Jones interaction energy versus time (0–10,000 ps) for choline: 6LU7 complex and presented in 3D Fig. 5a and Table 3. Energy values showed a stable nature up to 7000 ps of time scale data. Computed data revealed the less effect of binding affinity due to Coulombic interaction energy (-50.776 ± 20.12 kJ mol⁻¹) compared to Lennard-Jones interaction energy (-95.26 ± 22.10 kJ mol⁻¹). Time resolved variation of energy values are also found to match perfectly with the RMSDs of the complex for full time scale region.

To establish the stronger ligand binding affinities towards receptor we have applied the MM/PBSA method which deals with net free binding energy (ΔG) change as a sum of comprehensive set of energies of individual components. Molecular docking only suggests the binding energy of the complex while ΔG indicates the nonbonding interaction energies of the binding region for the complex formation. The average MM/PBSA free binding energy (ΔG_{bind}) of choline in complex was obtained as -33.497 kJ/mol which is good enough due to its well binding affinity towards SARS-CoV2 protease. The Van der Waal energy (E_{vdw}) component (-34.656 kJ/mol) also showed very good binding affinity of choline towards 6LU7 whereas electrostatic energy (E_{electrostatic}) did not show any significant role (-7.380 kJ/mol) in the complexation process. The variation of all energies needed for ΔG (energy in vacuum, polar and nonpolar solvation energies) is described in Fig. 5b. Fig. 5c shows the average free ΔG_{bind} in the whole-time trajectory. All the MD simulation results reported in this work and summarized above validate that choline can make an impressively stable complex with SARS-CoV2 protein after binding to the active sites of this 3CL^{PRO} protease.

4. Conclusion

CoV2 infection is anticipated to affect fetal development in a manner similar to other respiratory viruses which are known to be responsible for the maternal inflammatory response on the fetus and placenta. Earlier studies have established that if a mother gets infected by a respiratory coronaviruses during early pregnancy, higher prenatal choline level in her body can safeguard the developing brain of the fetus from the adverse effects of CoV2 infection. There are many natural resources of choline (e.g., vegetables, egg, milk, whole grains, herbal plants). Our ADME analysis (physiochemical, pharmacokinetics, drug

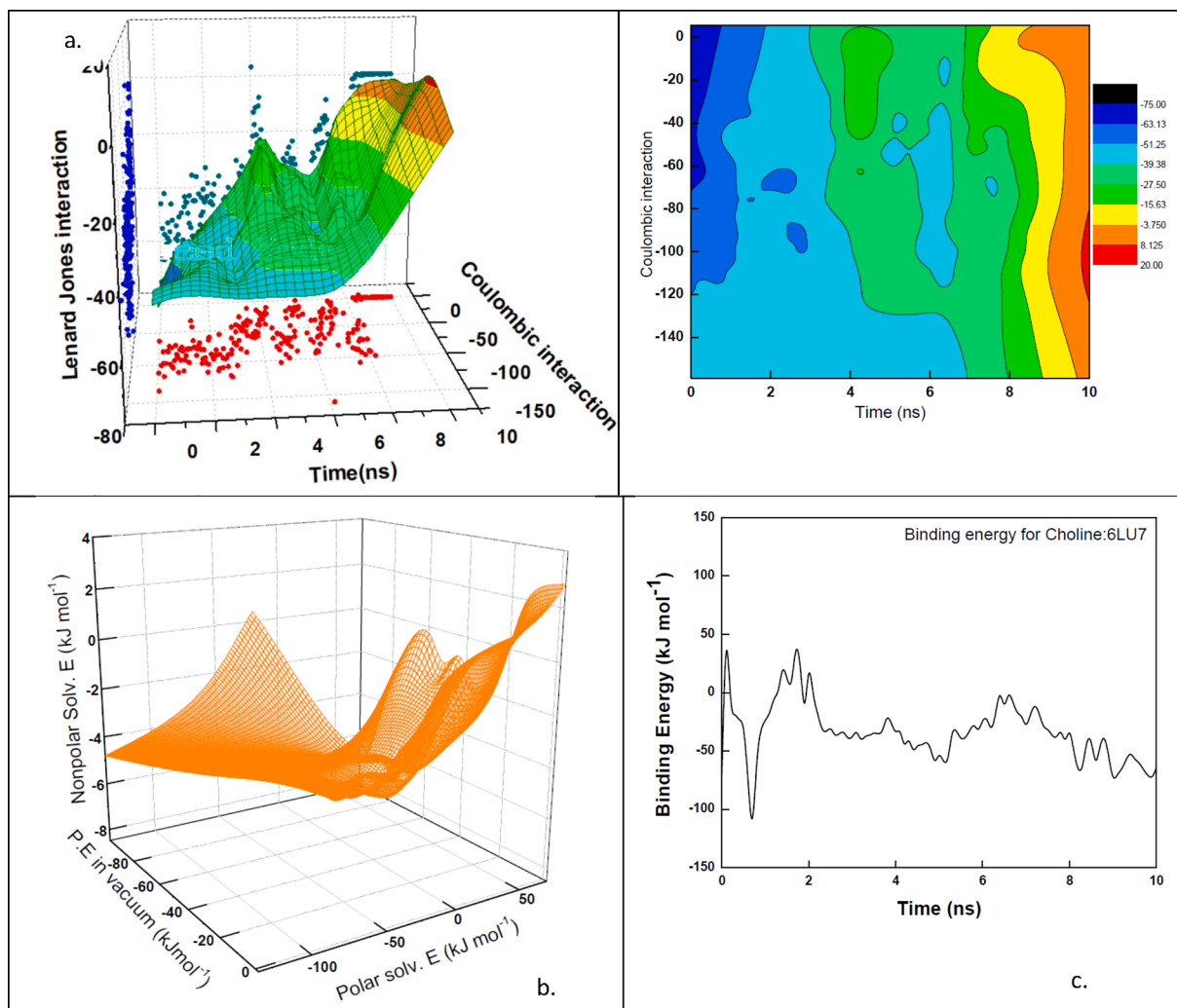


Fig. 5. For choline: 6LU7 complex: (a) Variation of Coulombic interaction energy and Lenard Jones interaction energy with respect to time (attached with color contour representation with specific color coding), (b) Relation between Energy in vacuum, Polar solvation energy, Nonpolar solvation energy, (c). Variation of total Free binding energy with respect to full time trajectory (0–10,000 ps).

likeness, medicinal chemistry) have found a strong inhibitory possibility of choline for SARS-CoV2 protease 3CL^{pro}. Molecular docking results with strong binding binding affinity, lowest inhibition constant and existence of hydrogen bonded interaction have established the possibility of existence of choline: 6LU7 complex structure. Various thermodynamic parameters (E_{pot} , T, V, D, R_g , SASA energy, interaction energies, ΔG_{bind}) obtained by Molecular dynamics simulation have validated the complexation between choline and CoV2 protein (6LU7). Summarizing all simulated output and interpreting their analysis have helped us to establish choline as a strong candidate to be used as a potential inhibitor for SARS-CoV2. We believe that our present *in silico* study would provide a lead for the prenatal drug development for the treatment of COVID-19. Still to efficiently target CoV2 infections, production of high quality concentrated choline extract and *in vivo*, *in vitro* experimental validation of the present work and clinical studies are defensible.

CRediT authorship contribution statement

Papia Chowdhury: Conceptualization, Formal analysis, Funding acquisition, Methodology, Validation, Project administration, Resources, Supervision, Visualization, Writing - review & editing, Writing - original draft, Methodology, Data curation, Investigation. **Pustak Pathak:** Data curation, Visualization, Investigation, Software.

Declaration of Competing Interest

The authors declare that they have no known competing financial interests or personal relationships that could have appeared to influence the work reported in this paper.

Appendix A. Supplementary material

Supplementary data to this article can be found online at <https://doi.org/10.1016/j.cplett.2020.138057>.

References

- [1] L. Hsuan Liang, L. Jin Chung, H. Yih, W.C. Chin, Homology models of main proteinase from coronavirus, *Chem. Phys. Lett.* 401 (2005) 24–29.
- [2] T. Estola, Coronaviruses, a new group of animal RNA viruses, *Avian Dis.* 14 (2) (1970) 330–336, <https://doi.org/10.2307/1588476>.
- [3] M. Kenneth, R.K. Chao, H.E. Krause, H.E. Krause, R. Wasil, H.E. Mocega, M.A. Mufson, Coronavirus infection in acute lower respiratory tract disease of infants, *J. Infect. Dis.* 130 (1974) 5.
- [4] S. Perlman, J. Netland, Coronaviruses post-SARS: update on replication and pathogenesis, *Nat. Rev. Microbiol.* 7 (6) (2009) 439–450, <https://doi.org/10.1038/nrmicro2147>.
- [5] P.A. Rota, M.S. Oberste, S.S. Monroe, W.A. Nix, R. Campagnoli, J.P. Icenogle, S. Peñaranda, B. Bankamp, K. Maher, M.-H. Chen, S. Tong, A. Tamin, L. Lowe, M. Frace, J.L. DeRisi, Q. Chen, D. Wang, D.D. Erdman, T.C.T. Peret, et al., Characterization of a novel coronavirus associated with severe acute respiratory

- syndrome, *Science* 300 (5624) (2003) 1394–1399, <https://doi.org/10.1126/science.1085952>.
- [6] S. Su, G. Wong, W. Shi, J. Liu, A.C. Lai, J. Zhou, et al., Epidemiology, genetic recombination, and pathogenesis of coronaviruses, *Trends Microbiol.* 24 (6) (2016) 490–502, <https://doi.org/10.1016/j.tim.2016.03.003>.
- [7] C. Huang, Y. Wang, X. Li, L. Ren, J. Zhao, Y. Hu, et al., Clinical features of patients infected with 2019 novel coronavirus in Wuhan, China, *Lancet* 395 (2020) 497–506.
- [8] N.C. Peeri, N. Shrestha, M.S. Rhaman, R. Zaki, Z. Tan, S. Bibi, M. Baghbanzadeh, N. Aghamohammadi, W. Zhang, U. Hague, The SARS, MERS and novel coronavirus (COVID-19) epidemics, the newest and biggest global health threats: what lessons have we learned? *Int. J. Epidemiol.* 20 (2020) 1–10.
- [9] A.E. Gorbelenya, S.C. Baker, R.S. Baric, R.J. de Groot, C. Drosten, A.A. Gulyaeva, B. L. Haagmans, C. Lauber, A.M. Leontovich, B.W. Neuman, D. Penzar, S. Perlman, L. L.M. Poon, D.V. Samborskiy, I.A. Sidorov, I. Sola, J. Ziebuhr, The species Severe acute respiratory syndrome-related coronavirus: classifying 2019-nCoV and naming it SARS-CoV-2, *Nature Microbiol.* (2020), <https://doi.org/10.1038/s41564-020-0695-z>.
- [10] <https://www.cdc.gov/coronavirus/2019-ncov/symptoms-testing/symptoms.html>.
- [11] N. Chen, M. Zhou, X. Dong, et al., Epidemiological and clinical characteristics of 99 cases of 2019 novel coronavirus pneumonia in Wuhan, China: a descriptive study, *Lancet* 395 (10223) (2020) 507–513, [https://doi.org/10.1016/S0140-6736\(20\)30211-7](https://doi.org/10.1016/S0140-6736(20)30211-7).
- [12] Y.-Y. Zheng, Y.-T. Ma, J.-Y. Zhang, X. Xie, COVID-19 and the cardiovascular system, *Nat. Rev. Cardiol.* 17 (5) (2020) 259–260, <https://doi.org/10.1038/s41569-020-0360-5>.
- [13] Johns Hopkins CSSE, Coronavirus COVID-19 (2019-nCoV), 2020. Retrieved July 18, 2020, from Coronavirus COVID-19 Global Cases by Johns Hopkins CSSE website: <https://gisanddata.maps.arcgis.com/apps/opsdashboard/index.html#/bda7594740fd40299423467b48e9ecf6>.
- [14] C.C. Gomez, et al., Clinical consensus recommendations regarding non-invasive respiratory support in the adult patient with acute respiratory failure secondary to SARS-CoV-2 infection, (2020), *Revista Española de Anestesiología y Reanimación* 67 (5) (2020) 261–270, <https://doi.org/10.1016/j.redare.2020.05.001>.
- [15] T.M. Pius, N.N. Koto te, S.T.T. Damien, T.K. Jason, Z.G. Benjamin, T.M. Domaine, L.I. Clement, M.L. Emmanuel, M.M. Clement, M. Aristote, N.B. Gedeon, D. T. Dorothee, Identification of potential inhibitors of SARS-CoV-2 main protease from Aloe vera compounds: a molecular docking study, *Chem. Phys. Lett.* 754 (2020).
- [16] N.W. Furukawa, J.T. Brooks, J. Sobel, Evidence supporting transmission of severe acute respiratory syndrome coronavirus 2 while presymptomatic or asymptomatic, *Emerg. Infect. Dis.* 26 (7) (2020), <https://doi.org/10.3201/eid2607.201595>.
- [17] Li Chunyang, et al., Asymptomatic and human-to-human transmission of SARS-CoV-2 in a 2-family cluster, Xuzhou, China, *Emerg. Infect. Dis.* 26 (7) (2020) 1626–1628, <https://doi.org/10.3201/eid2607.200718>.
- [18] I. Ghinai, et al., First known person-to-person transmission of severe acute respiratory syndrome coronavirus 2 (SARS-CoV-2) in the USA, *The Lancet* 395 (10230) (2020) 1137–1144, [https://doi.org/10.1016/S0140-6736\(20\)30607-3](https://doi.org/10.1016/S0140-6736(20)30607-3).
- [19] <https://www.msdmanuals.com/home/infections/respiratory-viruses/coronaviruses-and-acute-respiratory-syndromes-covid-19-mers-and-sars#>.
- [20] C. Chang, S.-C. Lo, Y.-S. Wang, M.-H. Hou, Recent insights into the development of therapeutics against coronavirus diseases by targeting N protein, *Drug Discovery Today* 21 (4) (2016) 562–572.
- [21] J. Grein, N. Ohmagari, D. Shin, G. Diaz, E. Asperges, A. Castagna, T. Feldt, Compassionate use of remdesivir for patients with severe Covid-19, *N. Engl. J. Med.* (2020) 1–10, <https://doi.org/10.1056/NEJMoa2007016>.
- [22] P. Suryapad, T.H. Chi, Y.S. Lee, Dietary therapy and herbal medicine for COVID-19 prevention: a review and perspective, *J. Tradit. Complement. Med.* 10 (4) (2020) 420–427.
- [23] K.G. Manoj, V. Sarojamma, D. Ravindra, G. Gyatri, B. Lambodar, V. Ramkrishna, In-silico approaches to detect inhibitors of the human severe acute respiratory syndrome coronavirus envelope protein ion channel, *J. Biomol. Struct. Dyn.* (2020), <https://doi.org/10.1080/07391102.2020.1751300>.
- [24] C. Papia, In silico investigation of phytoconstituents from indian medicinal herb ‘*Tinospora Cordifolia* (Giloy)’ against SARS-CoV-2 (COVID-19) by molecular dynamics approach, *J. Biomol. Struct. Dyn.* (2020), <https://doi.org/10.1080/07391102.2020.1803968>.
- [25] S.A. Mednick, R.A. Machon, M.O. Huttunen, D. Bonett, Adult schizophrenia following prenatal exposure to an influenza epidemic, *Arch. Gen. Psychiatr.* 45 (1988) 189–192.
- [26] J.W. Dreier, A.-M. Nybo Andersen, A. Hvolby, E. Garne, P.K. Andersen, G. Berg-Beckhoff, Fever and infections in pregnancy and risk of attention deficit/hyperactivity disorder in the offspring, *J. Child Psychol. Psychiatry* 57 (2016) 540–548.
- [27] S.A. Mednick, R.A. Machon, M.O. Huttunen, D. Bonett, Adult schizophrenia following prenatal exposure to an influenza epidemic, *Arch. Gen. Psychiatr.* 45 (1988) 189–192.
- [28] R. Freedman, S.K. Hunter, A.J. Law, B.D. Wagner, A. D’Alessandro, U. Christians, et al., Higher gestational choline levels in maternal infection protect infant brain development, *J. Pediatr.* 208 (2019), 198–206.e2.
- [29] B.T.F. Wu, R.A. Dyer, D.J. King, K.J. Richardson, S.M. Innis, Early second trimester maternal plasma choline and betaine are related to measures of early cognitive development in term infants, *PLoS ONE* 7 (8) (2012) e43448, <https://doi.org/10.1371/journal.pone.0043448>.
- [30] M. Zhang, X. Han, J. Bao, J. Yang, S.-Q. Shi, R.E. Garfield, H. Liu, Choline supplementation during pregnancy protects against gestational lipopolysaccharide induced inflammatory responses, *Reprod. Sci.* 25 (2018) 74–85.
- [31] C.J. Moore, M. Perreault, M.F. Mottola, S.A. Atkinson, Diet in early pregnancy: focus on folate, Vitamin B12, Vitamin D, and choline, *Can. J. Diet Pract. Res.* (2019), <https://doi.org/10.3148/cjdrp-2019-025>.
- [32] S. Pal, S. Pal, Understanding the role of reline, a natural DES, on temperature-induced conformational changes of C-Kit G-Quadruplex DNA: a molecular dynamics study, *J. Phys. Chem. B* 124 (15) (2020) 3123–3136, <https://doi.org/10.1021/acs.jpcb.0c00644>.
- [33] S. Pal, S. Pal, Effect of hydrated and nonhydrated choline chloride–urea deep eutectic solvent (reline) on thrombin-binding G-quadruplex Aptamer (TBA): a classical molecular dynamics simulation study, *J. Phys. Chem. C* 123 (18) (2019) 11686–11698, <https://doi.org/10.1021/acs.jpcc.9b01111>.
- [34] A. Maity, S. Sarkar, L. Theeyancheri, R. Chakrabarti, Choline chloride as a nanocrowder protects HP-36 from urea-induced denaturation: insights from solvent dynamics and protein-solvent interactions, *ChemPhysChem* 21 (2020) 552–567.
- [35] M. Hassan, R.H. Mohammad, Akbar M.M. Ali, R.B. Mohammad, How a protein can remain stable in a solvent with high content of urea: insights from molecular dynamics simulation of *Candida antarctica* lipase B in urea: choline chloride deep eutectic solvent, *Phys. Chem. Chem. Phys.* 16 (2014) 14882–14893, <https://doi.org/10.1039/C4CP00503A>.
- [36] S.H. Zeisel, Choline, in: A.C. Ross, B. Caballero, R.J. Cousins, K.L. Tucker, T.R. Ziegler (Eds.), Modern Nutrition in Health and Disease, 11th ed., Lippincott Williams & Wilkins, Baltimore, MD, 2014, pp. 416–426.
- [37] S.A. Mednick, R.A. Machon, M.O. Huttunen, D. Bonett, Adult schizophrenia following prenatal exposure to an influenza epidemic, *Arch. Gen. Psychiatry* 45 (2) (1988) 189–192.
- [38] CDC. Data on COVID-19 during Pregnancy. <https://www.cdc.gov/coronavirus/2019-ncov/cases-updates/special-populations/pregnancy-data-on-covid-19.html> (accessed June 29, 2020).
- [39] S. Canetta, A. Sourander, H.M. Surcel, et al., Elevated maternal C-reactive protein and increased risk of schizophrenia in a national birth cohort, *Am. J. Psychiatry* 171 (9) (2014) 960–968.
- [40] M. Zhang, et al., Choline supplementation during pregnancy protects against gestational lipopolysaccharide-induced inflammatory responses, *Reprod. Sci.* 25 (2018) 74–85.
- [41] H. Chen, J. Guo, C. Wang, et al., Clinical characteristics and intrauterine vertical transmission potential of COVID-19 infection in nine pregnant women: a retrospective review of medical records, *Lancet* 395 (10226) (2020) 809–815.
- [42] I. Jha, A. Rani, P. Venkatesu, Sustained stability and activity of lysozyme in choline chloride against pH induced denaturation, *ACS Sustain. Chem. Eng. ACS Sustain. Chem. Eng.* 5 (9) (2017) 8344–8355, <https://doi.org/10.1021/acssuschemeng.7b02126>.
- [43] S. Sarkar, S. Ghosh, R. Chakrabarti, Ammonium based stabilizers effectively counteract urea-induced denaturation in a small protein: insights from molecular dynamics simulations (2017), *RSC Adv.* 7 (2017) 52888–52906, <https://doi.org/10.1039/C7RA10712A>.
- [44] S. Apparsundaram, S.M. Ferguson, A.L. George Jr., R.D. Blakely, Molecular cloning of a human, hemicholinium-3-sensitive choline transporter, *Biochem. Biophys. Res. Commun.* 276 (2000) 862–867.
- [45] C.A. Lipinski, Lead- and drug-like compounds: the rule-of-five revolution, *Drug Disc. Today: Technol.* 1 (4) (2004) 337–341.
- [46] D.F. Veber, S.R. Johnson, H.Y. Cheng, B.R. Smith, K.W. Ward, K.D. Kopple, Molecular properties that influence the oral bioavailability of drug candidates, *J. Med. Chem.* 45 (12) (2002) 2615–2623.
- [47] A. Daina, O. Michielin, V. Zoete, SwissADME: a free web tool to evaluate pharmacokinetics, drug-likeness and medicinal chemistry friendliness of small molecules, *Sci. Rep.* 7 (2017) 42717, <https://doi.org/10.1038/srep42717>.
- [48] F.S. Michel, Python: a programming language for software integration and development, *J. Mol. Graphics Mod.* 17 (February) (1999) 57–61.
- [49] M. Marina, P. Marco, P. Piero, Identification of potential binders of the main protease 3CLpro of the COVID-19 via structure-based ligand design and molecular modeling, *Chem. Phys. Lett.* 750 (2020) 137489.
- [50] K. Anand, J. Ziebuhr, P. Wadhwanji, J.R. Mesters, R. Hilgenfeld, Coronavirus main protease (3CLpro) structure: basis for design of anti-SARS drugs, *Science* 300 (5626) (2003) 1763–1767.
- [51] T.P. Velavan, C.G. Meyer, The COVID-19 epidemic, *Tropical Med. Int. Health: TM & IH* 25 (3) (2020) 278–280, <https://doi.org/10.1111/tmi.13383>.
- [52] Z. Jin, X. Du, Y. Xu, Y. Deng, M. Liu, Y. Zhao, B. Zhang, X. Li, L. Zhang, C. Peng, Y. Duan, J. Yu, L. Wang, K. Yang, F. Liu, R. Jiang, X. Yang, T. You, X. Liu, H. Yang, Structure of Mpro from COVID-19 virus and discovery of its inhibitors, *Nature* (2020), <https://doi.org/10.1038/s41586-020-2223-y>.
- [53] O. Trott, A.J. Olson, AutoDock Vina: improving the speed and accuracy of docking with a new scoring function, efficient optimization, and multithreading, *J. Comput. Chem.* 31 (2) (2010) 455–461, <https://doi.org/10.1002/jcc.21334>.
- [54] Dassault Systèmes BIOVIA, Discovery Studio Modeling Environment, Release 2017, San Diego: Dassault Systèmes.
- [55] E. Yuriev, M. Agostino, P.A. Ramsland, Challenges and advances in computational docking: 2009 in review, *J. Mol. Recognit.* 24 (2011) 149–164.
- [56] H.J.C. Berendsen, D. van der Spoel, R. van Drunen, GROMACS: a messagepassing parallel molecular dynamics implementation, *Comput. Phys. Commun.* 91 (1–3) (1995) 43–56.
- [57] I. Soteras Gutierrez, F.-Y. Lin, K. Vanommeslaeghe, J.A. Lemkul, K.A. Armacost, Cl. Brooks III, A.D. MacKerell Jr., Parametrization of halogen bonds in the

- CHARMM general force field: improved treatment of ligand-protein interactions, *BioorganicMed. Chem.* (2016), <https://doi.org/10.1016/j.bmc.2016.06.034>.
- [58] W.F. van Gunsteren, S.R. Billeter, A.A. Eising, P.H. Hünenberger, P. Krüger, A.E. Mark, W.R.P. Scott, I.G. Tironi, *Biomolecular simulation: The GROMOS96 manual and user guide*. Hochschulverlag AG an der ETH Zürich, Zürich, Switzerland, 1996.
- [59] A. Becke, A new inhomogeneity parameter in density-functional theory, *J. Chem. Phys.* 107 (1997) 8554, <https://doi.org/10.1063/1.476722>.
- [60] M.J. Frisch, *Gaussian 09, revision D.01*; Gaussian Inc.: Wallingford CT, 2004.
- [61] K. Rashmi, K. Rajendra, L. Andrew, g_mmmpbsa—a GROMACS tool for high-throughput MM-PBSA calculations, *J. Chem. Inf. Model.* 54 (7) (2014) 1951–1962, <https://doi.org/10.1021/ci500020m>.
- [62] P.A. Kollman, I. Massova, C. Reyes, B. Kuhn, S.H. Huo, L. Chong, et al., Calculating structures and free energies of complex molecules: combining molecular mechanics and continuum models, *Acc. Chem. Res.* 33 (2000) 889–897, <https://doi.org/10.1021/ar000033j>.
- [63] W. Changhao, G. D'Artagnan, X. Li, Q. Ruxi, L. Ray, Recent developments and applications of the MMPSA method, *Front. Mol. Biosci.* (2018), <https://doi.org/10.3389/fmolb.2017.00087>.
- [64] Swiss ADME: a free web tool to evaluate pharmacokinetics, drug-likeness and medicinal chemistry friendliness of small molecules. *Sci. Rep.* 7 (2017) 42717.
- [65] L.M. Stephen, et al., DREIDING: a generic force field for molecular simulations, (1990), *J. Phys. Chem.* 94 (26) (1990) 8897–8909, <https://doi.org/10.1021/j100389a010>.
- [66] R. Patil, S. Das, A. Stanley, L. Yadav, A. Sudhakar, A.K. Varma, Optimized Hydrophobic interactions and hydrogen bonding at the target-ligand interface e pathways of drug-designing, *PLoS One* 5 (8) (2016) e12029.
- [67] M. Leonardo, Automatic identification of mobile and rigid substructures in molecular dynamics simulations and fractional structural fluctuation analysis, *PLoS ONE* 10 (3) (2015) e0119264.
- [68] K.Y. Dharmendra, et al., Molecular insights into the interaction of RONS and Thieno[3,2-c]pyran analogs with SIRT6/COX-2: a molecular dynamics study, *Scientific RePORTS* 8 (2018) 4777, <https://doi.org/10.1038/s41598-018-22972-9>.
- [69] S.A. Khan, K. Zia, S. Ashraf, R. Uddin, Z. Ul-Haq, Identification of chymotrypsin-like protease inhibitors of SARS-CoV-2 via integrated computational approach, *J. Biomol. Struct. Dyn.* (2020) 1–10, <https://doi.org/10.1080/07391102.2020.1751298>.
- [70] A.E. Abodo, SARS-CoV-2 RNA dependent RNA polymerase (RdRp) targeting: an in silico perspective, *J. Biomol. Struct. Dyn.* (2020), <https://doi.org/10.1080/07391102.2020.1761882>.